Bioprocess Biosyst Eng (2017) 40:791–796
DOI 10.1007/s00449-017-1744-8

RESEARCH PAPER

Metabolic engineering of *Synechocystis* sp. PCC 6803 for enhanced ethanol production based on flux balance analysis

Katsunori Yoshikawa[1] · Yoshihiro Toya[1] · Hiroshi Shimizu[1]

Received: 21 September 2016 / Accepted: 24 January 2017 / Published online: 3 March 2017

Abstract *Synechocystis* sp. PCC 6803 is an attractive host for bio-ethanol production due to its ability to directly convert atmospheric carbon dioxide into ethanol using photosystems. To enhance ethanol production in *Synechocystis* sp. PCC 6803, metabolic engineering was performed based on in silico simulations, using the genome-scale metabolic model. Comprehensive reaction knockout simulations by flux balance analysis predicted that the knockout of NAD(P)H dehydrogenase enhanced ethanol production under photoautotrophic conditions, where ammonium is the nitrogen source. This deletion inhibits the re-oxidation of NAD(P)H, which is generated by ferredoxin-$NADP^+$ reductase and imposes re-oxidation in the ethanol synthesis pathway. The effect of deleting the *ndhF1* gene, which encodes NADH dehydrogenase subunit 5, on ethanol production was experimentally evaluated using ethanol-producing strains of *Synechocystis* sp. PCC 6803. The ethanol titer of the ethanol-producing Δ*ndhF1* strain increased by 145%, compared with that of the control strain.

Keywords Ethanol production · Flux balance analysis · Genome-scale metabolic model · *NdhF1* deletion · *Synechocystis* sp. PCC 6803

✉ Hiroshi Shimizu
shimizu@ist.osaka-u.ac.jp

[1] Department of Bioinformatic Engineering, Graduate School of Information Science and Technology, Osaka University, 1-5 Yamadaoka, Suita, Osaka 565-0871, Japan

Introduction

Cyanobacteria are attractive hosts for bio-production, because they can directly convert atmospheric carbon dioxide into target chemicals using photosystems. Deng and Coleman introduced two *Zymomonas mobilis* genes, *pdc* and *adhII* (encoding pyruvate decarboxylase and alcohol dehydrogenase, respectively) into *Synechococcus elongates* PCC 7942, and successfully produced 0.23 g L^{-1} of ethanol—a widely used bio-fuel [1]. Cyanobacterial ethanol production has been improved in *Synechocystis* sp. PCC 6803 (hereafter, PCC 6803) via various strategies, such as promoter selections for the heterologous genes [2], inhibition of by-product formations [3], two-phase cultivation with nutrient starvation [4], and excess NADPH production by over-expression of *zwf* encoding glucose-6-phosphate dehydrogenase [5]. Although Gao et al. achieved 5.5 g L^{-1} of ethanol production within 26 d by engineering the expression of ethanol synthesis pathway enzymes and by disrupting a by-product synthesis pathway [3], further improvements are required for practical applications. While engineering based on intuitive strategies has been conducted, a comprehensive prediction at the system level must provide new perspectives.

In many fermentation microorganisms, the redox balance in the metabolism of the whole cell is also important for efficient bio-production [6]. Computer simulation is a powerful tool for metabolic design that takes whole cell metabolism into consideration. Flux balance analysis (FBA) is a method for predicting flux distribution based on reaction stoichiometry, using linear programming with an objective function, such as biomass yield maximization [7]. FBA has been used to predict genetic engineering targets that can enhance production of specific substances. Gene knockouts have been explored to force target production for

growing well [7]. Owing to the rapid nature of the computation time for FBA simulation, it is possible to perform comprehensive in silico screening using a large-scale model. Although many success stories have been reported in fermentation microorganisms [8], the application of FBA techniques to bio-production in cyanobacteria has been limited.

There are several reported genome-scale metabolic models of PCC 6803 [9, 10]. A model developed by Yoshikawa et al. simulated flux distributions that were consistent with data obtained from experiments that used ^{13}C-labeling [11]. Here, metabolic flux changes caused by reaction knockouts were simulated by FBA, using the genome-scale metabolic model. This was performed to identify gene deletion candidates that could enhance ethanol production. The accuracy of these in silico predictions was experimentally evaluated in ethanol-producing PCC 6803 strains.

Materials and methods

Strain construction

The *Synechocystis* sp. PCC 6803 glucose-tolerant strain was used as the host strain. The *ndhF1* deletion strain (*Δ*ndhF1) was constructed in previous studies [12]. Ethanol-producing strains were constructed by introducing *pdc* and *adhII* genes from *Z. mobilis* based on the ethanol production of PCC 6803 by Dexter and Fu [13]. Due to the sever growth inhibition, *pdc* and *adhII* genes were controlled by the *nblA* promoter, into the neutral site of the PCC 6803 genome, as described in our previous report [14]. The *nblA* promoter, the *pdc* gene, and the *adhII* gene were obtained from the pNdhB–nblAp–EtOH plasmid construct [14] by *Xho*I and *Bam*HI digestion, and were cloned into the *Xho*I and *Bam*HI sites of the pSlr0168–psbA2p–me–Sm plasmid construct [14]. The resulting vector, pSlr0168–nblAp–EtOH–Sm, containing the homologous region for slr0168 and the streptomycin resistance gene, was introduced into the neutral site inside slr0168 [15] of the genomes of the PCC 6803 and ΔndhF1 strains (subsequently named 6803/EtOH and *Δ*ndhF1/EtOH, respectively). For transformation, 1 μg of the plasmid DNA was mixed with 1 mL of culture (with OD_{730} of approximately 0.5). After 2 h of incubation under light at 34 °C, the mixtures were applied to a 0.22 μm pore-sized membrane filter (Millipore) on BG11 plates without antibiotic. After overnight incubation under light at 34 °C, the membrane filters were moved to BG11 plates supplemented with 20 μg streptomycin mL^{-1}. The obtained transformants were repeatedly streaked on BG11 plates with streptomycin until complete segregation occurred. The transformation was confirmed by colony PCR using the primer pair 5′-CCCATCGTAAAATTCGTTCC-3′ and 5′-CTGGTG TAAATTCGCAAACG-3′, which bound to the upstream and downstream regions of slr0168 based on size disparities of the PCR products. The strains used in this study are shown in Table 1.

Culture condition

Pre-culture was performed autotrophically in 100 mL Erlenmeyer flasks with 20 mL modified BG11 medium [13], at 34 °C, with rotary agitation at 150 rpm (BR-43FL shaker; TAITEC Co., Ltd., Japan), and under continuous illumination (40 μmol m^{-2} s^{-1}) by white light-emitting diodes (LC-LED450W, TAITEC Co., Ltd., Japan). The culture medium was supplemented with appropriate antibiotics, such as streptomycin (10 μg mL^{-1}) and erythromycin (5 μg mL^{-1}). The pre-cultivated cells were harvested by centrifugation, and were then inoculated into the modified BG11 medium containing 5 mM NH_4Cl in place of $NaNO_3$ as a nitrogen source without antibiotics at an OD_{730} of 0.03. The main culture was performed under 100 μmol m^{-2} s^{-1} at 34 °C.

Flux balance analysis

A genome-scale metabolic model of PCC 6803 was used in this study [11]. The following ethanol synthetic pathway was added to the model:

$$\text{Pyruvate[c]} \Leftrightarrow \text{Acetaldehyde[c]} + CO_2\text{[c]}$$
$$\text{Acetaldehyde[c]} + \text{NADPH[c]} \rightarrow \text{Ethanol} + NADP^+\text{[c]}$$
$$\text{Acetaldehyde[c]} + \text{NADH[c]} \rightarrow \text{Ethanol[c]} + NAD^+\text{[c]}$$
$$\text{Ethanol[c]} \Leftrightarrow \text{Ethanol[e]}$$

where [c] and [e] denote intra- or extracellular metabolite, respectively. An objective function for optimal growth was used for the flux estimation by the linear programming

Table 1 Strains used in this study

Strain	Relevant genotype[a]	References
PCC 6803	*Synechocystis* sp. PCC 6803, glucose tolerant	
ΔndhF1	*ndhF1*::Em^r	Ogawa et al. [12]
6803/EtOH	NS::P_{nblA}–*pdc–adh*, Sm^r	This study
ΔndhF1/EtOH	*ndhF1*::Em^r, NS::P_{nblA}–*pdc–adh*, Sm^r	This study

[a]NS, neutral site inside slr0168 [15]; Em^r, erythromycin resistance gene; Sm^r, streptomycin resistance gene

technique. The photon uptake rate was set to a given value to simulate an autotrophic condition. The uptake rates of ammonia or nitrate as nitrogen sources were unrestricted. The export fluxes for amino acids were set to zero. The metabolic flux changes caused by knockouts of all possible combinations of any three reactions from the model were simulated under this condition.

To reveal the ethanol-biomass solution space, the maximum and minimum fluxes of ethanol production were calculated, using an objective function as the maximization or minimization of ethanol production, with each fixed growth rate from zero to the maximum value [16]. The ethanol production rate and the growth rate were converted to carbon yields using coefficient 2 C-mol mol $^{-1}$ and 36.89 C-mmol gDCW^{-1}, respectively. All calculations were performed using MATLAB R2011b and GLPK software (GNU Linear Programming Kit).

Analytical method

The cell concentration of the culture was measured by optical density using a spectrophotometer at 730 nm (OD_{730}) (UVmini-1240, Shimadzu, Kyoto, Japan). The biomass amount was calculated from OD_{730} using an experimentally determined conversion coefficient (0.3 g dry cell weight $OD_{730}{}^{-1}$ L^{-1}). Gas chromatography, with a hydrogen flame ionization detector (7890 A; Agilent Technologies, CA, USA) and a Stabiliwax column (0.32 mm internal diameter, 60 m length, and 1 μm thickness; Restek, PA, USA), was used to measure the ethanol concentration of the culture broth. The inlet temperature was set to 250 °C. The column oven temperature was initially set at 70 °C for 3 min, and was then increased to 200 °C at 10 °C min^{-1}. 3-methyl-1-butanol was used as an internal standard for quantification.

The yields of biomass and ethanol were calculated between 0 and 288 h of culture time. The carbon content of the biomass was assumed to be 36.89 C-mmol gDCW^{-1}, based on the biomass component of the genome-scale model.

Results and discussion

In silico design of optimal metabolic pathway for ethanol production

The flux distribution was simulated by FBA using an objective function for maximization of biomass synthesis based on the genome-scale metabolic model of PCC 6803 with ethanol synthetic reactions. Ammonia or nitrate was set as a nitrogen source. The metabolic flux changes caused by knockouts of all possible combinations of any three reactions from the model of PCC 6803 were simulated to identify sets of reaction knockouts for enhancing ethanol production. These simulations predicted that a triple reaction knockout strain produces ethanol at the maximum growth yield under the ammonia condition. No knockout candidate was predicted under the nitrate condition:

$$\text{R055(cytochrome oxidase):}2H + 0.5O_2 + QH_2 \rightarrow 2H[t] + H_2O + Q$$

$$\text{R567(NADH dehydrogenase):}NADH + 5H + Q \rightarrow 4H[t] + NAD^+ + QH_2$$

$$\text{R568(NADPH dehydrogenase):}NADPH + 5H + Q \rightarrow 4\,H[t] + NADP^+ + QH_2$$

where [t] denotes metabolite at the thylakoid lumen. Q and QH_2 denote ubiquinone and ubiquinol, respectively.

Because the selected reactions are all related to the respiratory chain, it was suggested that inhibition of the electron flow enhances ethanol production. The biomass and ethanol yields of the control and the triple reaction knockout (hereafter referred to as ΔR055–ΔR567–ΔR568) strains are summarized in Table 2.

The metabolic state of the ΔR055–ΔR567–ΔR568 strain should be restricted to ethanol production, coupled with cell growth, by the knockouts. In other words, the knockout strain must produce ethanol to generate its cellular components. To investigate the relationship between cell growth and ethanol production, stoichiometrically feasible ranges of ethanol production yield were calculated at each biomass yield, based on mass balances (Fig. 1). The gray area within Fig. 1 represents the feasible ethanol yield at each biomass yield in the control strain. Because the maximization of biomass yield was used as an objective function for FBA simulation, the predicted metabolic state corresponds to the point of the open circle symbol in Fig. 1. The feasible range of ethanol yield was restricted to the shaded area in the ΔR055–ΔR567–ΔR568 strain due to the additional gene knockout constraints. The predicted metabolic state of the ΔR055–ΔR567–ΔR568 strain by FBA is located on the point of the open square symbol. The lower limit of the feasible ethanol yield in this strain increases with respect to increases in biomass yield. This means that ethanol production is coupled to biomass production.

Table 2 Result of gene knockout simulations for ethanol production in PCC 6803

Knockout	Biomass yield (C-mol/C-mol-CO_2)	Ethanol yield (C-mol/C-mol-CO_2)
None	1.00	0.00
ΔR055–ΔR567–ΔR568	0.14	0.86

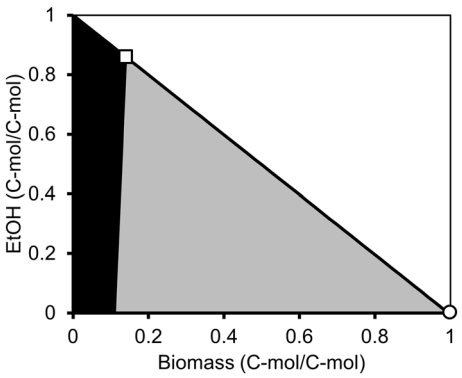

Fig. 1 Ethanol-biomass solution space of the parent strain and its ΔR055–ΔR567–ΔR568 strain. *Black* and *gray areas* represent feasible range of ethanol yield against biomass yield for the control and its ΔR055–ΔR567–ΔR568 strain, respectively. *Open circle* and *open square symbols* represent the FBA-predicted metabolic states of parent and its ΔR055–ΔR567–ΔR568 strain, respectively

No ethanol production at the maximum cell growth state was predicted in the ΔR055–ΔR567–ΔR568 strain under the nitrate condition. Nitrate is reduced to ammonium by ferredoxin-nitrate reductase and ferredoxin-nitrite reductase. Because eight moles of ferredoxin are oxidized per 1 mol of nitrate in these reactions, ferredoxin-NADP$^+$ reductase can re-oxidize NADPH, using the oxidized ferredoxin. Therefore, ethanol was not produced under the nitrate condition, due to the absence of any excess NADPH production.

To reveal the mechanism for enhancing ethanol production via reaction knockouts, the flux distributions on the metabolic pathways in the control, ΔR055, and ΔR055–ΔR567–ΔR568 strains are shown in Fig. 2. The strains transfer electrons from water to plastoquinone (PQ) via photosystem II (PSII), using photons as the energy supply. Electrons are transferred through the electron transport chain, including PSI, and are used for NADPH generation by ferredoxin-NADP$^+$ reductase (FNR). In the parent strain, some of the electrons in PQ are transferred to oxygen by cytochrome oxidase (Cyd). NADPH generation by

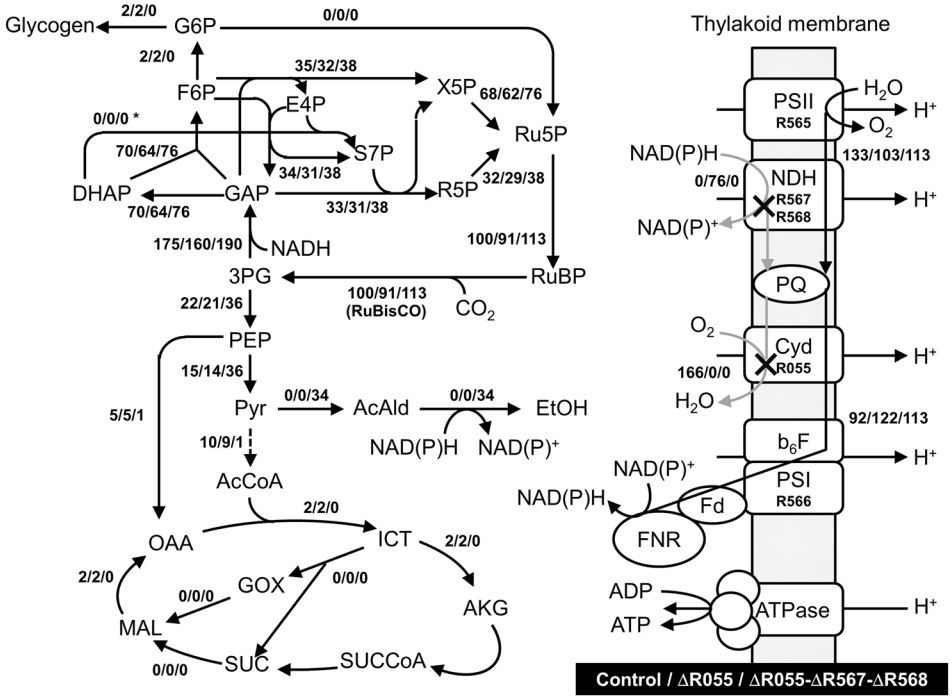

Fig. 2 Simulated flux distributions of control strain and its deletion strains. Values represent the metabolic flux, which is normalized to the flux of ribulose 1,5-bisphosphate carboxylase/oxygenase (RuBisCO) as 100, of the control strain. The fluxes of control (*right*), ΔR055 strain (*middle*), and ΔR055–ΔR567–ΔR568 strain (*right*), are separated by a *slash*. *To choose a unique solution, an infinitesimally negative weight for this flux was added to the objective function, to avoid the undetermined flux of this reaction. *G6P* glucose 6-phosphate, *F6P* fructose 6-phosphate, *DHAP* dihydroxyacetone phosphate, *GAP* glyceraldehyde 3-phosphate, *3PG* 3-phosphoglycerate, *PEP* phosphoenolpyruvate, *Pyr* pyruvate, *AcCoA* acetyl-CoA, *Ru5P* ribulose 5-phosphate, *RuBP* ribulose 1,5-bisphosphate, *R5P* ribose 5-phosphate, *X5P* xylulose 5-phosphate, *E4P* erythrose 4-phosphate, *S7P* sedoheptulose 7-phosphate, *ICT* isocitrate, *AKG* α-ketoglutarate, *SUCCoA* succinyl-CoA, *SUC* succinate, *MAL* malate, *OAA* oxaloacetate, *GOX* glyoxylate, *AcAld* acetaldehyde, *PSII* photosystem II, *NDH* NAD(P)H dehydrogenase, *PQ* plastoquinone, *Cyd* cytochrome oxidase, *PSI* photosystem I, *Fd* ferredoxin, *FNR* ferredoxin-NADP reductase

FNR increases with increasing flux through the electron transport chain, including PSI, in the ΔR055 strain. Excess NADPH for growth is re-oxidized by NAD(P)H dehydrogenase (NDH). In the ΔR055–ΔR567–ΔR568 strain, ethanol is synthesized to re-oxidize the excess NADPH.

Although no flux of the NDH reaction was predicted by FBA in the control strain, it has been reported that cell growth defects were caused by the deletion of genes encoding NDH in PCC 6803 [17, 18]. This inconsistency between simulation outcomes and experimental observations suggests the existence of the NDH flux in the control strain. NDH works to re-oxidize NADPH, which is produced via the PSI in the case of decreasing Cyd flux. Therefore, the actual Cyd flux must be restricted to a value smaller than that predicted by FBA. To accomplish more realistic simulations, feasible ethanol yields against biomass yields were simulated by limiting the Cyd flux to 100, 70, 40, and 0% of that of the control strain, with NDH deletions (Fig. 3). Figure 3 indicates that ethanol is produced by the only deletion of the NDH reaction with the restricted Cyd flux.

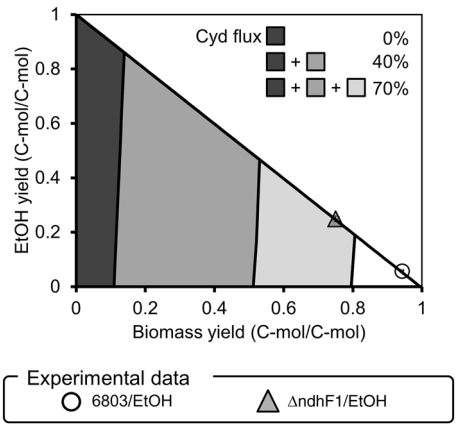

Fig. 3 Effects of cytochrome oxidase flux on ethanol production

Evaluation of ethanol productivity in NADH dehydrogenase deletion strain

The effect of deleting NDH from the PCC 6803 genome on ethanol production was experimentally evaluated. A knockout mutant of the *ndhF1* gene, which encodes NADH dehydrogenase subunit 5, was used as the NDH deletion strain. Because the coenzyme specificity of this enzyme is unclear in PCC 6803, two reactions (NADH-dependent and NADPH-dependent) were considered in the model. Therefore, the *ndhF1* deletion constitutes a double-knockout of both NADH dehydrogenase and NADPH dehydrogenase. The genes for *pdc* and *adh* from *Z. mobilis* were introduced into the PCC 6803 and ΔndhF1 strain. These strains were cultured under photoautotrophic conditions, with ammonium as a nitrogen source. The cell growth and ethanol production for these strains are shown in Fig. 4. Growth of the 6803/EtOH strain (control) continued for 12 d, and 132 mg ethanol L^{-1} was produced in 14 days. As expected, growth of the ΔndhF1/EtOH strain decreased after 6 days, while ethanol production rates increased. The ethanol titer of the ΔndhF1/EtOH strain increased by 145% compared to that of the control strain. Growth rates and ethanol production rates changed after 6 days. This could be explained by the decrease of Cyd flux during the experimental time period, because the optimal metabolic state can change depending on the Cyd flux in the ΔndhF1/EtOH strain (Fig. 3). Control of the Cyd flux should be effective for achieving optimal cell growth and ethanol production. A two-phase culture would be useful to achieve high titer production of ethanol. After growth using glucose, a high cell density culture should be used for ethanol production, with slight growth under autotrophic conditions using ammonium as the nitrogen source.

To compare experimental results and the simulation that was based on the genome-scale model, the measured yields of biomass and ethanol were plotted on the ethanol-biomass solution space in Fig. 3. The amounts of biomass and ethanol produced between 0 and 288 h of culture time were

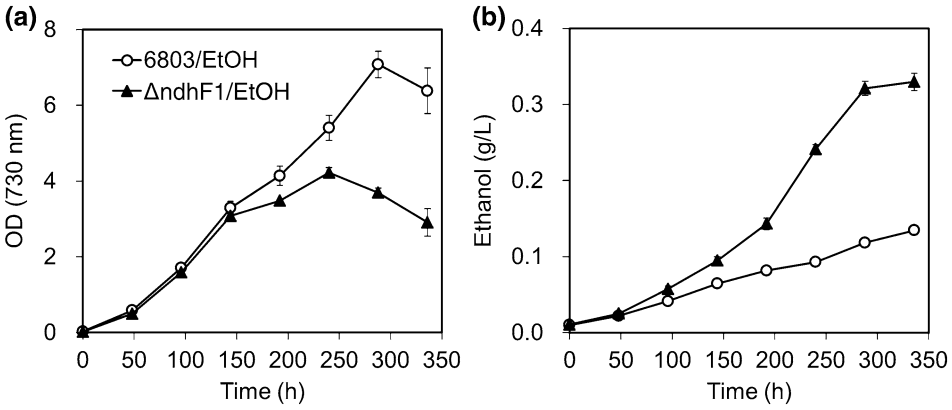

Fig. 4 Cell growth (**a**) and ethanol production (**b**) of the 6803/EtOH and ΔndhF1/EtOH strains. *Circles* and *triangles* represent the 6803/EtOH and ΔndhF1/EtOH strains, respectively

calculated. It has been assumed that CO_2 uptake was only utilized for biomass and ethanol production. Because the measured biomass yield exceeded the simulated range in the case of no Cyd flux (Fig. 3), this suggests the existence of Cyd flux in the ΔndhF1/EtOH strain. Therefore, deletion or inhibition of Cyd could potentially further enhance the ethanol yield.

Furthermore, the cyclic electron flow (CEF) reaction is not included in this model. The simulation considering the CEF reaction must be required an additional knockout of the CEF reaction for ethanol production, because the reaction can consume electron for ATP production without NADPH generation. For the same reason as the Cyd flux, the enhanced ethanol production was observed without CEF deletion, because the flux is restricted to a certain value in practice.

Conclusions

In this study, we first experimentally demonstrated the application of an *in silico* metabolic design that was based on a genome-scale metabolic model for ethanol production in PCC 6803. In alcohol production using fermentation microorganisms, such as *E. coli*, cells are cultured under anaerobic conditions to inhibit oxidative phosphorylation. In our experiments, metabolic pathways were altered to use the reductive power generated in glycolysis to generate the target product. Therefore, strains that were knockouts of the fermentation pathways were intended to enhance ethanol production in the cells. However, the anaerobic strategy is not feasible in PCC 6803, because oxygen production in cyanobacteria is inevitable under the autotrophic conditions. Here, we found a new strategy: NDH deletion leads to increased ethanol production, based on in silico simulations. This deletion inhibits the re-oxidation of NAD(P)H, which is generated by ferredoxin-$NADP^+$ reductase, and imposes re-oxidation in the ethanol synthesis pathway. We experimentally confirmed that this deletion can successfully enhance ethanol production in *Synechocystis* sp. PCC 6803. This knockout strategy would be useful not only for the production of ethanol, but also for the production of various metabolites in cyanobacteria that require reductive power for synthesis.

Acknowledgements We would like to thank Prof. Sonoike (Waseda University) for providing the ΔndhF1 strain of PCC 6803. This work was supported by Grant in Aid for Scientific Research (A) No. 24246134. This work was also supported by JSPS KAKENHI Grant Number 16H06559.

References

1. Deng MD, Coleman JR (1999) Ethanol synthesis by genetic engineering in cyanobacteria. Appl Environ Microbiol 65:523–528
2. Dexter J, Armshaw P, Sheahan C, Pembroke JT (2015) The state of autotrophic ethanol production in Cyanobacteria. J Appl Microbiol 119:11–24
3. Gao ZX, Zhao H, Li ZM, Tan XM, Lu XF (2012) Photosynthetic production of ethanol from carbon dioxide in genetically engineered cyanobacteria. Energ. Environ Sci 5:9857–9865
4. Namakoshi K, Nakajima T, Yoshikawa K, Toya Y, Shimizu H (2016) Combinatorial deletions of *glgC* and *phaCE* enhance ethanol production in *Synechocystis* sp. PCC 6803. J Biotechnol 10:13–19
5. Choi YN, Park JM (2016) Enhancing biomass and ethanol production by increasing NADPH production in *Synechocystis* sp. PCC 6803. Bioresour Technol 213:54–57
6. Chen X, Li S, Liu L (2014) Engineering redox balance through cofactor systems. Trends Biotechnol 32:337–343
7. Feist AM, Zielinski DC, Orth JD, Schellenberger J, Herrgard MJ, Palsson BO (2010) Model-driven evaluation of the production potential for growth-coupled products of *Escherichia coli*. Metab Eng 12:173–186
8. Simeonidis E, Price ND (2015) Genome-scale modeling for metabolic engineering. J Ind Microbiol Biotechnol 42:327–338
9. Knoop H, Zilliges Y, Lockau W, Steuer R (2010) The metabolic network of *Synechocystis* sp. PCC 6803: systemic properties of autotrophic growth. Plant Physiol 154:410–422
10. Montagud A, Navarro E, Fernández de Córdoba P, Urchueguía JF, Patil KR (2010) Reconstruction and analysis of genome-scale metabolic model of a photosynthetic bacterium. BMC Syst Biol 4:156
11. Yoshikawa K, Kojima Y, Nakajima T, Furusawa C, Hirasawa T, Shimizu H (2011) Reconstruction and verification of a genome-scale metabolic model for *Synechocystis* sp. PCC 6803. Appl Microbiol Biotechnol 92:347–358
12. Ogawa T, Harada T, Ozaki H, Sonoike K (2013) Disruption of the *ndhF1* gene affects Chl fluorescence through state transition in the Cyanobacterium *Synechocystis* sp. PCC 6803, resulting in apparent high efficiency of photosynthesis. Plant Cell Physiol 54:1164–1171
13. Dexter J, Fu P (2009) Metabolic engineering of cyanobacteria for ethanol production. Energy. Environ Sci 2:857–864
14. Yoshikawa K, Hirasawa T, Shimizu H (2015) Effect of malic enzyme on ethanol production by *Synechocystis* sp. PCC 6803. J Biosci Bioeng 119:82–84
15. Angermayr SA, Paszota M, Hellingwerf KJ (2012) Engineering a cyanobacterial cell factory for production of lactic acid. Appl Environ Microbiol 78:7098–7106
16. Wada K, Toya Y, Banno S, Yoshikawa K, Matsuda F, Shimizu H (2016) ^{13}C-metabolic flux analysis for mevalonate-producing strain of *Escherichia coli*. J Biosci Bioeng. doi:10.1016/j.jbiosc.2016.08.001
17. Ohkawa H, Pakrasi HB, Ogawa T (2000) Two types of functionally distinct NAD(P)H dehydrogenases in *Synechocystis* sp. strain PCC6803. J Biol Chem 275:31630–31634
18. Ohkawa H, Price GD, Badger MR, Ogawa T (2000) Mutation of *ndh* genes leads to inhibition of CO_2 uptake rather than HCO_3^- uptake in *Synechocystis* sp. strain PCC 6803. J Bacteriol 182:2591–2596